Delayed Gamma Rays from Photofission of U^{238}, U^{235}, and Th^{232} *

R. B. WALTON, R. E. SUND, E. HADDAD, AND J. C. YOUNG
General Atomic Division of General Dynamics Corporation, John Jay Hopkins Laboratory for Pure and Applied Science, San Diego, California

AND

C. W. COOK†
North American Aviation Incorporated, El Segundo, California

(Received 1 November 1963)

Absolute delayed gamma-ray intensities from the photofission of U^{238}, U^{235}, and Th^{232} were measured as a function of time after bursts of fissions produced by the bombardment of samples with 20-MeV x rays from an electron linear accelerator. For all three target nuclei, components of short-lived gamma rays, which are attributed to the decay of isomers formed either in fission or, less likely, by other photoreactions, contributed markedly to the gamma-ray activity for times up to 800 μsec after the beam pulse. Beyond 800 μsec the gamma-ray activity decreased little for times up to about 10^{-1} sec. The gamma rays emitted in this interval, the "plateau" region, and at longer times are believed to follow beta decay of fission fragments. In the "plateau" region, the absolute intensities of gamma rays ($E_\gamma > 0.51$ MeV) from the photofission of U^{238}, U^{235}, and Th^{232} are 0.70, 0.26, and 0.35 photons/fission-sec, respectively. After 0.1 sec the gamma-ray decay curves have the same shapes as those observed by other investigators in neutron fission of the same target nuclei, but the absolute intensity from photofission is approximately a factor of two less than that from neutron fission.

INTRODUCTION

UNTIL a few years ago, very little experimental data on delayed gamma rays from the gross aggregate of fission products had been reported, particularly for times less than 100 sec after fission.[1] Fisher and Engle,[2] using a fast multiplying assembly (GODIVA II) as a pulsed source of neutrons, recently completed a study of gamma rays from the fast neutron fission of Th^{232}, U^{233}, U^{235}, U^{238}, and Pu^{239} over the time interval from 0.2 to 45 sec after fission. Maienschein, Peelle, Zobel, and Love[3] have measured delayed gamma rays from the thermal neutron fission of U^{235} for times from 1 to 1800 sec by irradiating samples in a reactor and then transferring them pneumatically to gamma-ray spectrometers. The latter workers also investigated the time interval from 5 nsec to 1 μsec by time-analyzing gamma-ray signals following individual fission events in a U^{235} fission chamber which was placed in a beam of thermal neutrons. Results of a similar experiment have recently been reported by Desi, Latjtai and Nagy.[4]

The present paper is concerned with measurements of delayed gamma rays from fission for times ranging from a few microseconds to 10 sec, a time region of particular interest because of the possibility of observing two different effects in the time behavior of the gamma-ray intensity. The first effect pertains to gamma rays following the beta decay of fission fragments. Since beta decay is in general an important process only for nuclear excitation energies less than the neutron binding energy, the shortest allowed beta-ray transitions should have half-lives of the order of 0.1 sec. Hence, for times appreciably less than this, the activity of the gamma rays associated with beta decay of fission fragments should show almost no time dependence.[5] On the other hand, the decay of short-lived isomers formed directly in fission could cause the delayed gamma-ray intensity to decrease rapidly with time, an effect which might be expected for fission because of the great abundance of short-lived isomers observed in other reactions.[6,7]

APPARATUS

A pulsed beam of x rays for causing photofissions was produced by bombarding a tungsten target with 20-MeV electrons from a linear accelerator. Instantaneous electron beam currents up to 400 mA were available within a $\frac{1}{2}$-cm spot at the target position, and the duration of the electron beam was variable from 10 nsec to 5 μsec. The bremsstrahlung x rays were collimated through a 5-cm hole in a 2.4-m-thick shield wall, beyond which were located beam monitors, samples, and the gamma-ray detector. A schematic drawing of this configuration is shown in Fig. 1. The x-ray beam was monitored with a plastic scintillator mounted on an ITT photodiode tube, the current from which was proportional to the intensity of x rays traversing the scintillator. The 12.8-h β^+ activity from $Cu^{65}(\gamma,n)Cu^{64}$ reactions induced in copper foils which were placed in the beam served as

* This research is a part of Project DEFENDER, sponsored by the Advanced Research Projects Agency, Department of Defense, under Contract AF 29(601)-5373.

† Work initiated while the author was at General Dynamics/Convair, San Diego, California.

[1] J. E. Brolley, D. H. Cooper, W. S. Hall, M. S. Livingston, and L. K. Slacks, Phys. Rev. **83**, 990 (1951).

[2] P. C. Fisher and L. B. Engle, Phys. Rev. first preceding paper, **134**, B796 (1964).

[3] F. C. Maienschein, R. W. Peelle, W. Zobel, and T. A. Love, Proc. 2nd Intern. Conf. Peaceful Uses At. Energy **15**, 366 (1958).

[4] S. Desi, A. Latjtai, and L. Nagy, Acta. Acad. Sci. Hung. **15**, 185 (1962).

[5] K. Way and E. P. Wigner, Phys. Rev. **73**, 1318 (1948).

[6] A. W. Schardt, Phys. Rev. **122**, 1871 (1961).

[7] H. Krehbiel and U. Meyer-Berkhout, Z. Physik **167**, 99 (1961).

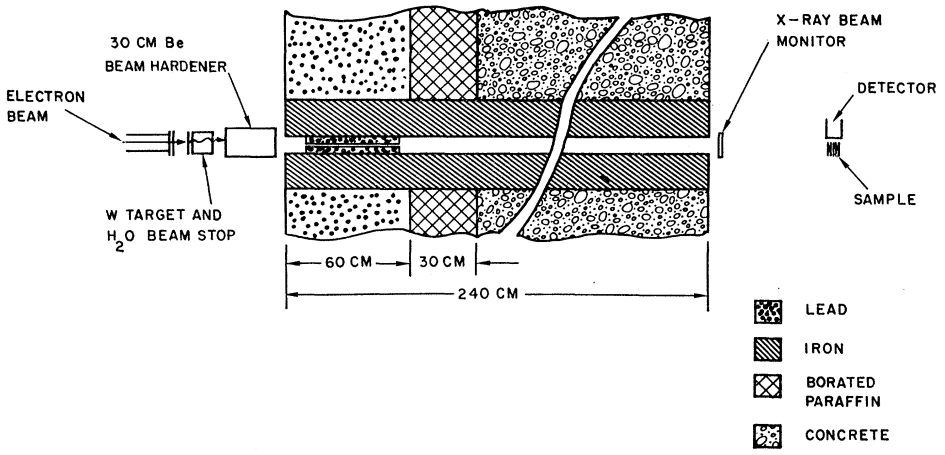

FIG. 1. Experimental configuration.

an additional monitor. A single beam pulse produced a maximum of approximately 5×10^3 fissions per gram of U^{238} at the sample position.

Ten identical samples were mounted on a rotating aluminum holder which triggered the accelerator each time a sample arrived in the beam path. The highest beam repetition rate that could be utilized without generating excessive background activity in the samples was 1 pulse per second. For the study of the time region beyond 0.1 sec, a single sample, fixed in the beam path, was bombarded at a rate of 1 pulse per min.

The detector and samples were enclosed in a shielding cage having large openings for the passage of the x-ray beam. The walls of the cage, which were approximately 75 cm apart, consisted of 5 cm of lead and an inside liner of boron-paraffin 7.5 cm thick. This shielding proved very effective for times greater than 100 μsec after the beam pulse but was removed for measurements at earlier times because of the gamma-ray background generated by scattering and absorption of neutrons by the enclosure.

Figure 2 is a sketch of the detector and sample geometry. Each sample consisted of four identical units spaced 1.2 cm apart to reduce the self-absorption of gamma rays. The detector for gamma rays consisted of a plastic scintillator (Pilot B), 5 cm in diameter and 2.54 cm thick, mounted on a 10-stage EMI photomultiplier tube. (Although NaI has better properties for gamma-ray detection, it could not be used in this experiment because of the intensity of the long-lived phosphorescence[8] produced by the "beam flash," primarily bremsstrahlung x rays scattered from the samples into the detector.) To expedite recovery of the photomultiplier gain after the overloading signal from the beam flash, a relatively small total resistance, 7×10^4 Ω, was used in the bleeder string distributing high voltage to the photomultiplier dynodes. A piece of borated polyethylene, 2.5 cm thick, was attached in front of the scintillator to stop beta rays and to attenuate neutrons from the samples.

Signals from the gamma-ray detector were passed through a cathode follower to an amplifier especially designed for stable performance over a wide range of counting rates and pulse heights.[9] Pulses from the integral bias discriminator output of the amplifier were fed to two 256-channel time analyzers, which were usually triggered ahead of the beam pulse by several time channels to measure the activity of the sample immediately preceding the burst of fissions. Channel widths used for this study ranged from 2 μsec to 3.2×10^{-2} sec.

To check the performance of the detection system under beam conditions, decay rates of gamma rays from isomeric transitions produced by (γ,n) reactions in lead and bismuth were measured and the half-lives obtained from these data agreed very well with previously reported[10] values, i.e., 132 μsec for lead and 2.7 msec for bismuth. Furthermore, the time required for the detection system to recover from beam-flash effects, as well as the subsequent gain stability of the system, was investigated as a function of beam intensity with a thick tungsten sample placed in the beam and a Co^{60}

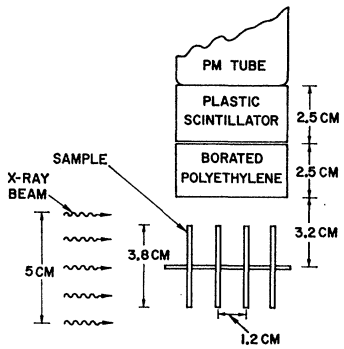

FIG. 2. Detector and sample geometry.

[8] H. M. Barton and C. F. Cook, Bull. Am. Phys. Soc. **7**, 112 (1962).

[9] G. G. Kelly, IRE Natl. Conv. Record **9**, 63 (1959).

[10] Stanley H. Vegors, Jr., and Peter Axel, Phys. Rev. **101**, 1067 (1956).

source located near the detector. Measurements of the time dependence of the Co^{60} gamma rays, which were much more intense than background radiations, yielded the recovery times and showed that the system was

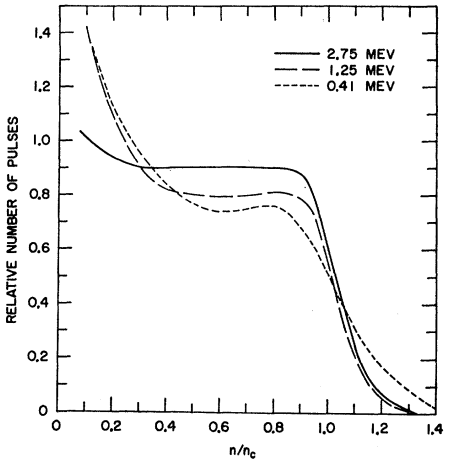

FIG. 3. Gamma-ray pulse-height distributions of the plastic scintillation detector presented in the form of normalized response functions. The abscissa is the ratio of channel number (n) to the channel number (n_c) corresponding to E_c, and the scale of the ordinate was fixed by normalizing the area under each curve to unity.

stable throughout the remainder of the time between beam pulses.

The energy calibration of the detector was made relative to the Compton edges of pulse-height distributions taken with several standard gamma-ray sources. In terms of the photon energy E_γ, the energy of the Compton peak or the maximum single-collision energy transfer E_c is given by $E_\gamma[1+(m_0c^2)/(2E_\gamma)]^{-1}$, where m_0c^2 is the electron rest energy. The assignment of E_c to the pulse height at which the intensity of pulses had fallen to approximately two-thirds of its value at the "Compton peak" gave a linear relationship for pulse height versus E_c for gamma rays from sources covering the energy range from 0.32 to 2.75 MeV. A few of the pulse-height distributions are presented in Fig. 3 in the form of normalized response functions of the detector.

The detector efficiency was determined experimentally for integral bias settings of 0.25 and 0.51 MeV using calibrated sources placed at the position of the fission sample. Corrections for the geometrical sizes of the sources and fission samples were negligible when the distance between a sample and the detector was measured from center to center. Measured efficiencies for the 0.51-MeV bias are indicated by points in Fig. 4.

To fit the measured efficiencies with a smooth curve and to provide a basis for extrapolating to 6 MeV, the efficiency was calculated as the product of the solid angle subtended by the detector, the attenuation by the borated polyethylene shield, the total number of single gamma-ray interactions occuring in the plastic scintillator, and the biasing fraction. This last, which is the fraction of pulses falling above the discriminator bias, was determined from pulse-height distributions. As may be seen in Fig. 4, the calculated efficiencies for the 0.51-MeV bias agree with the measured points for gamma-ray energies up to about 0.9 MeV, above which they are lower by approximately 15%. This difference was probably caused by multiple gamma-ray interactions in the polyethylene and the scintillator. For energies above 0.9 MeV, the calculated curve for the 0.51-MeV bias was normalized to the experimental data; the final efficiency curve used for data analysis is given by the solid curve in Fig. 4.

Factors to account for the self-absorption of gamma rays by the relatively thick fissionable samples required for this experiment were obtained from measurements of the absorption of gamma rays from sources interlaced between thin lead foils to simulate the sample disks shown in Fig. 2. The self-absorption factor, or the ratio of counting rates from the sources with lead to those from sources without lead, was determined as a function of the thickness of lead in each disk for three gamma-ray energies, 0.41, 0.74, and 1.6 MeV. For integral discriminator bias settings above 0.25 MeV, the self-absorption factors were, to within a few percent, independent of the bias. The lead thickness (in g/cm²) was then multiplied by the ratio of the total gamma-ray absorption coefficients of uranium (or thorium) and lead to obtain the equivalent g/cm² of uranium (or thorium). This procedure should be valid, because the energy dependence and absolute values of the absorption coefficients for these elements are quite similar.

The resulting experimental self-absorption factors for the thickness of U^{238} used in this study, 2.94 g/cm² per disk, are given by the points in Fig. 5. The solid curve shown in this figure was simply drawn through the points at 0.41 and 0.74 MeV, while the extrapolation to higher energies was made with the expression for the transmission of gamma rays emitted from a thin sample

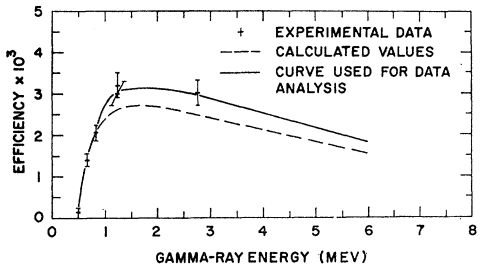

FIG. 4. Gamma-ray detector efficiency for an integral bias of 0.51 MeV. The solid angle subtended by the detector is contained implicitly in the efficiencies shown.

perpendicular to the plane of the sample, $(1/l\mu_u)[1-\exp(-l\mu_u)]$, where l is the sample thickness and μ_u is the total gamma-ray absorption coefficient of uranium. Although this formula is not strictly applicable to

the present geometry, l may be pictured as a "mean disk radius" which gamma rays must penetrate before being detected. The expression was fitted to the experimental point at 1.6 MeV by using ℓ as a free parameter; the results are given by the dashed curve in Fig. 5. This extrapolation should be sufficiently accurate for the energy range between 1.2 and 6 MeV because the samples are relatively thin for gamma rays of these energies and μ_u changes little with energy. The broken curve in Fig. 5 represents μ_u as a function of gamma-ray energy.

Similarly, the self-absorption factors were derived for the U^{235} and the Th^{232} samples, the thicknesses of which were 0.893 and 2.45 g/cm^2 per disk, respectively. For the U^{235} samples, the self-absorption factors at 0.41, 0.74, and 1.6 MeV were 0.72±0.05, 0.77±0.04, and 0.89±0.03, respectively, while the corresponding quantities for the Th^{232} samples were 0.52±0.04, 0.63±0.03, and 0.80±0.02.

MEASUREMENTS

From 10^3 to 10^4 beam pulses were required to obtain good counting statistics for a delayed gamma-ray measurement for times up to 0.1 sec after the beam pulse; for longer times, approximately 10^2 beam pulses sufficed.

Backgrounds which were subtracted from the data consisted of the natural activity of the samples, the activity induced in each sample by preceding pulses, ambient background, and the background from neutrons. Except for the last of these, the backgrounds could be determined in a straightforward manner. Neutrons produced by (γ,F) and (γ,n) reactions in the fissionable samples caused a gamma-ray background that was comparable to the delayed gamma-ray signal and persisted until 15 msec after the beam pulse. Measurements with a tungsten sample, which served as a neutron source by means of (γ,n) reactions, were used to determine the neutron-induced background. Relative neutron yields from the tungsten and fissionable samples were determined from measurements with a BF_3 neutron detector embedded in a cadmium-covered block of paraffin. Because of 0.375-MeV gamma rays from a tungsten (γ,n) isomer, this method of evaluating the neutron background for the delayed gamma-ray data with 0.25-MeV bias could not be used directly for times less than about 100 μsec after the beam pulse. For this case, data with 0.51-MeV bias were normalized to the 0.25-MeV data at approximately 100 μsec, and it was assumed that the shape of the neutron background was the same for both biases.

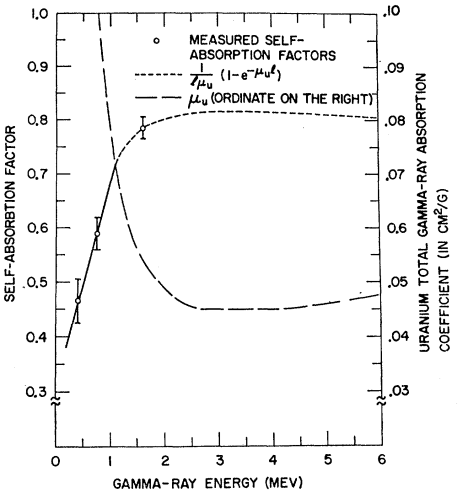

FIG. 5. Self-absorption factor as a function of gamma-ray energy for U^{238} samples (disk thickness = 2.94 g/cm^2). Also shown is the total gamma-ray absorption coefficient of uranium.

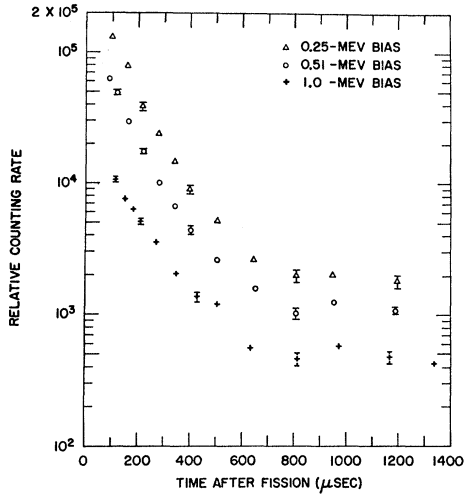

FIG. 6. U^{238} delayed gamma-ray counting rates recorded with integral bias settings of 0.25, 0.51, and 1.0 MeV. The statistical uncertainties of the measurements are indicated by the error bars.

Typical delayed gamma-ray data obtained from the photodisintegration of U^{238} by 20-MeV bremsstrahlung x rays are shown in Fig. 6, where relative counting rates are given as a function of time for three discriminator bias settings—0.25, 0.51, and 1.0 MeV. The apparent half-life of the intense short-lived component derived from the data with the 1-MeV bias was 80±10 μsec, while the data obtained with the lower biases gave 75±5 μsec. After approximately 800 μsec, the counting rates remained almost constant for times up to a few tenths of a second. For the sake of brevity the time region between 800 μsec and 0.1 sec may, in the remainder of this paper, be referred to as the "plateau" region, while the range of times up to 800 μsec is called the "isomeric" region.

Several U^{238} photoreactions other than (γ,F) have appreciable yields for bremsstrahlung x rays with an end point of 20 MeV and could therefore have been responsible for the delayed gamma rays shown in Fig. 6. To gain some information on the reactions responsible for these gamma rays, a single measurement was performed

using 11.6-MeV bremsstrahlung x rays, which produce only (γ,F) and (γ,n) reactions copiously. The 75-μsec delayed gamma-ray component was observed, and the ratio of its intensity to that in the plateau region was

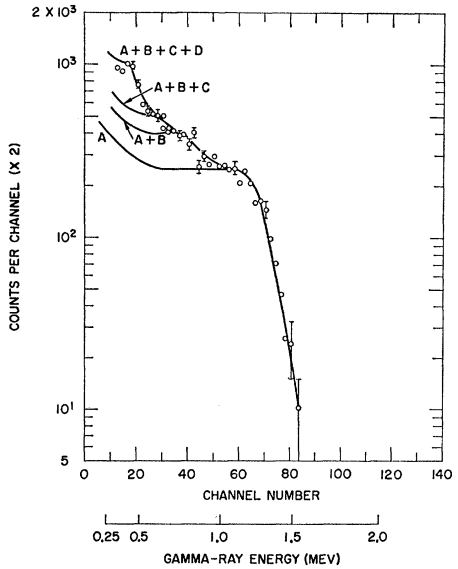

FIG. 7. Pulse-height distribution of delayed gamma rays emitted between 162 and 362 μsec after fission. The smooth curves show how the data were fitted with four gamma rays. The gamma-ray energy scale is given as an abscissa as well as the pulse height (channel number).

only slightly less than the corresponding ratio for the data taken with the 20-MeV beam. These results indicate that U^{238} photoreactions other than (γ,F) or (γ,n) are not responsible for the delayed gamma rays.

Further information on the U^{238} gamma-ray energy spectrum in the isomeric time region was obtained from a pulse-height distribution of gamma rays emitted between 162 and 362 μsec after the beam pulse. The integral bias measurements shown in Fig. 6 indicate that the spectral composition of gamma rays changes little during this time period. The experimental results of the pulse-height distribution measurement are shown by the points in Fig. 7, and the indicated errors reflect statistical uncertainties in the data. These data were corrected for backgrounds and, in addition, for those gamma rays associated with the plateau component of the decay on which the isomeric decays were superposed. The correction for the plateau component was determined from a pulse-height distribution of the pulses occuring between 1 and 10 msec after the beam pulse. Also shown in Fig. 7 are the results of an attempt to fit the experimental distribution with a number of gamma rays, which are denoted by A, B, etc. Self-absorption factors, detector efficiencies, and response functions were used for this "stripping" procedure. A minimum of four gamma rays was required to fit the experimental data. The energies of these gamma rays are 1.22, 0.84, 0.64, and 0.45 MeV, and their relative intensities are 1.00, 0.37, 0.24, and 0.71, respectively. Only the identification of the gamma ray with the highest energy is unambiguous; and the accuracy of this energy measurement is ± 0.05 MeV.

Figure 8 shows the pulse-height distribution of delayed gamma rays from $U^{238}(\gamma,F)$ emitted during the interval from 1 to 10 msec. The experimental data are represented by points, and a calculated pulse-height distribution, which was normalized to the experimental data at a pulse height corresponding to a 1-MeV gamma ray, is represented by the solid curve. These data differ markedly from the pulse-height distribution taken in the isomeric time region, and no discrete gamma-ray energies were discernible. The calculation of the pulse-height distribution was performed using the spectrum of delayed gamma rays from the neutron fission of U^{238}, which was measured at 0.35 sec after fission by Fisher and Engle.[2] This spectrum was divided into 17 energy groups, and the pulses each of these would produce in the plastic scintillation detector were sorted according to pulse height using the appropriate self-absorption factors and detector properties. It is apparent from Fig. 8 that the Fisher-Engle spectrum produces a good fit to the experimental data except for gamma-ray energies of less than 0.5 MeV, where the differences are well within the uncertainties in the detector efficiency and self-absorption factors used for the calculation. Such good agreement might be expected if the delayed gamma-ray spectra for $U^{238}(\gamma,F)$ and $U^{238}(n,F)$ are quite similar and if each spectrum is approximately inde-

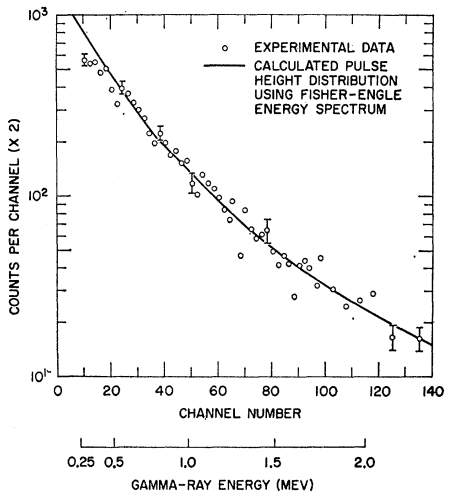

FIG. 8. Pulse-height distribution of delayed gamma rays emitted between 10^{-3} and 10^{-2} sec after fission. The gamma-ray energy scale is given by the lower abscissa.

pendent of time over the range from milliseconds to 0.35 sec. Both of these conditions are physically quite reasonable, and, in particular, the latter condition is fulfilled because the initial fission fragment populations

are not greatly depleted during this time interval (see the decay curves in Fig. 9). In addition, Fisher and Engle found that the delayed gamma-ray spectra change very little over the time range from 0.2 to 10 sec.

The intensities of delayed gamma rays from U^{238} and U^{235} were measured with 0.25- and 0.51-MeV bias settings for the time range from 100 μsec to 7 sec after photofission. For the Th^{232} measurements, only the 0.51-MeV bias was used. These counting-rate data were then converted to absolute gamma-ray intensities, Y_b (in units of photons per fission-sec), for gamma rays having energies greater than the bias energy E_b by the following expressions:

$$Y_b = R_b/FI_b$$

and

$$I_b = \int_{E_b}^{\infty} N_\gamma(E)\mathfrak{A}(E)\epsilon_b(E)dE \Big/ \int_{E_b}^{\infty} N_\gamma(E)dE,$$

where R_b = observed counting rate with bias E_b expressed as counts/sec for each beam pulse divided by the number of monitor counts per beam pulse, F = number of fissions per monitor count, $N_\gamma(E)$ = energy spectrum of gamma rays, $\mathfrak{A}(E)$ = self-absorption factor, $\epsilon_b(E)$ = detector efficiency with bias E_b.

The gamma-ray energy spectra for the neutron fission of U^{238}, U^{235}, and Th^{232}, which were measured by Fisher and Engle[2] at 0.35 sec after fission, were used for $N_\gamma(E)$ for times greater than about 800 μsec after fission. For earlier times, the isomeric component was separated from the plateau level, converted to absolute intensity, and then recombined with the absolute intensity of the

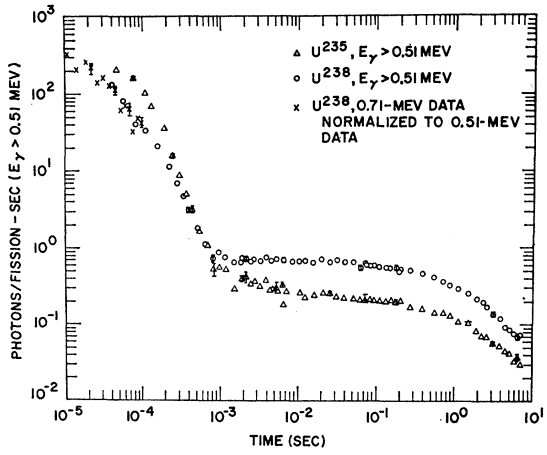

FIG. 9. Delayed gamma rays from the photofission of U^{238} and U^{235}. The number of photons per fission-sec having energies greater than 0.51 MeV is presented as a function of time after fission. Data for U^{235} were corrected for the effect of U^{238} (7%) present in the samples.

plateau region. The gamma-ray spectrum which fitted the pulse-height distribution measured for U^{238} in the isomeric region (shown in Fig. 7) was assumed for the conversion to absolute intensities for the isomeric components of U^{235} and Th^{232} as well as U^{238}. Because of the energy dependence of $\mathfrak{A}(E)$ and $\epsilon_b(E)$, this assumption could, of course, lead to errors if the spectrum depends on time and on the nuclide undergoing fission. These

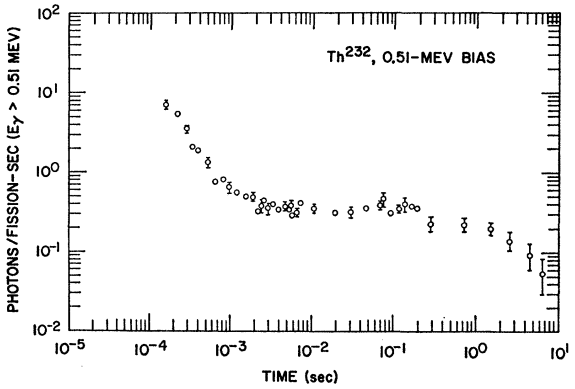

FIG. 10. Delayed gamma rays from the photofission of Th^{232}. The number of photons per fission-sec having energies greater than 0.51 MeV is presented as a function of time after fission.

errors would be larger for spectrum changes involving low-energy gamma rays. Integral bias data for U^{238}, given in Fig. 6, show that no significant changes in the fraction of low-energy gamma rays occur over a large portion of the isomeric region.

From an irradiation of a U^{238} sample and a subsequent determination of the yield of 17-h Zr^{97} by radiochemical analysis, the number of U^{238} fissions per monitor count F was determined. The value used for the Zr^{97} yield from U^{238} photofission with a 20-MeV bremsstrahlung spectrum was 5.75%. Previous work of Huizenga *et al.*[11] on the photofissionabilities of Th^{232} and U^{235} relative to U^{238} was used to obtain F for these nuclides.

TABLE I. Absolute delayed gamma-ray intensities (E_γ>0.51 MeV).

	Y(photons/fission-sec)			Y(photons/fission-sec)	
t(sec)	U^{238}	U^{235}	t(sec)	U^{238}	U^{235}
1×10^{-5}	340		2×10^{-3}	0.70	0.36
2×10^{-5}	217		3×10^{-3}	0.70	0.35
3×10^{-5}	152		4×10^{-3}	0.70	0.32
4×10^{-5}	112		6×10^{-3}	0.70	0.28
6×10^{-5}	70	200	8×10^{-3}	0.70	0.27
8×10^{-5}	50	166	1×10^{-2}	0.70	0.26
1×10^{-4}	38	116	2×10^{-2}	0.68	0.245
1.5×10^{-4}	22.3	57	4×10^{-2}	0.66	0.228
2×10^{-4}	14.8	29	8×10^{-2}	0.61	0.215
3×10^{-4}	6.25	8.60	1×10^{-1}	0.59	0.210
4×10^{-4}	3.10	3.70	2×10^{-1}	0.54	0.195
5×10^{-4}	1.85	2.03	4×10^{-1}	0.46	0.165
6×10^{-4}	1.30	1.27	8×10^{-1}	0.35	0.133
7×10^{-4}	1.04	0.90	1×10^{0}	0.31	0.122
8×10^{-4}	0.89	0.71	2×10^{0}	0.21	0.082
9×10^{-4}	0.80	0.58	3×10^{0}	0.15	0.061
1×10^{-3}	0.75	0.51	4×10^{0}	0.112	0.049
1.5×10^{-3}	0.70	0.39	7×10^{0}	0.064	0.031

[11] J. R. Huizenga, G. E. Gindler, and R. B. Duffield, Phys. Rev. **95**, 1009 (1954).

Figure 9 shows the absolute intensities of delayed gamma rays from U^{238} and U^{235} for energies greater than 0.51 MeV, and Fig. 10 gives the result for thorium. Data points for U^{235} and U^{238} were smoothed, and the results

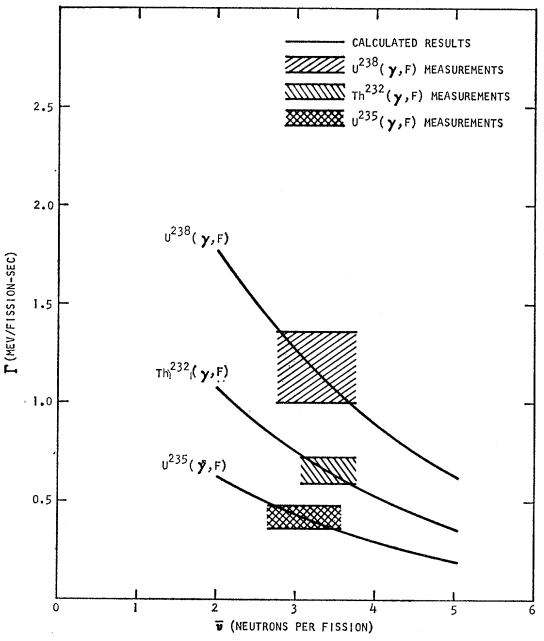

FIG. 11. Delayed gamma-ray energy emission rate Γ versus neutron multiplicity $\bar{\nu}$ for photofission of U^{238}, U^{235}, and Th^{232}. For comparison, the present experimental results are also shown.

are listed in Table I. For times less than 45 μsec following the beam pulse, the data shown for U^{238} were taken with a 0.7-MeV bias and then normalized to the data taken with 0.51-MeV bias in the vicinity of 75 μsec. For this normalization the assumption was made that the shapes of the decay curves for these bias settings were the same. The error bars in Figs. 9 and 10 indicate only the statistical uncertainties of the measurements. In the case of Th^{232}, these were relatively large because of the neutron background from (γ,n) reactions, which occurred much more frequently than photofissions, and because of the high natural activity of the thorium samples. The rms value of the significant uncertainties common to all the measurements is $\pm 15\%$ and comprises $\pm 10\%$ uncertainty in the detector efficiency, $\pm 6\%$ in self-absorption factors, $\pm 5\%$ in the reproducibility of the bremsstrahlung x-ray monitor, and $\pm 7\%$ in the radiochemical determination of the Zr^{97} yield from the irradiation of the U^{238} sample. Other significant errors may be present in the data for the isomeric time region because of the gamma-ray energy spectra which were assumed for the data reduction. A systematic error in all the data would arise if the Zr^{97} fission yield is different from the value used in the data reduction. Furthermore, the absolute intensities for U^{235} and thorium depend on the accuracy of the previous determination[11] of the photofissionabilities of these nuclides relative to U^{238}.

For both U^{235} and U^{238}, the absolute intensity of gamma rays with $E_\gamma > 0.25$ MeV was larger than that for $E_\gamma > 0.51$ MeV by a factor of 1.2 ± 0.1 over the time range from 1.5×10^{-4} sec to 7 sec. Since this factor is particularly sensitive to variations in the gamma-ray energy spectrum at low energies, it appears that such variations were small and that the assumptions made concerning the energy spectra used in the data reduction were valid.

DISCUSSION

As may be seen from Figs. 9 and 10, the gamma-ray decay curves for U^{238}, U^{235}, and Th^{232} are qualitatively quite similar. For times between 200 and 600 μsec after fission, the gamma-ray intensities for all three decay with approximately the same half-life, about 75 μsec. Since it is improbable that other reactions competing with (γ,F) for the three different target nuclei would lead to the same mode of decay, the gamma rays emitted during this period very likely result from the decay of several isomers formed during the fission process. This conclusion is also supported by the complexity of the pulse height distribution for U^{238} shown in Fig.7. Additional isomers with half-lives less than 100 μsec are indicated by the U^{238} data in the time region from 10 to 100 μsec.

For decay times less than 200 μsec, the intensity of gamma rays from the photodisintegration of U^{235} is much higher than those from U^{238} and thorium. This portion of the decay curve for U^{235} is dominated by a component consisting of one or more gamma rays with energies greater than 0.51 MeV and decaying with an apparent half-life of 40 ± 10 μsec. This component may result from a reaction other than (γ,F); however, the fission yield of a single isomer necessary to produce this activity is approximately 2%, which, for a wide range of fission product masses, is well within the limits imposed by the fission product mass-yield curve.[12] The decay curve for U^{235} also exhibits a component having a characteristic decay period of a few milliseconds, which is not apparent in the U^{238} data.

Because of the time dependence of the decay curves shown in Figs. 9 and 10 and their marked similarity for times greater than 10^{-2} sec, these gamma rays are almost certainly associated with the beta decay of fission fragments. The present observation that the absolute intensity of delayed gamma rays depends strongly on the target nucleus is consistent with the findings of Fisher and Engle[2] for the fast-neutron fission of several nuclides.

Griffin[13] has formulated a procedure for correlating the delayed gamma-ray intensity in the plateau and

[12] R. B. Duffield, R. A. Schmitt, and R. A. Sharp, Proc. 2nd Intern. Conf. Peaceful Uses At. Energy **15**, 202 (1958).

[13] James Griffin, Phys. Rev. **134**, B817 (1964), second preceding paper.

long-time regions for any arbitrary case of neutron fission to the results[2] measured for the fast-neutron fission of U^{235}. His theory is based on the average beta-decay properties of the fission fragments, which are governed by the initial displacement of the fragments from the line of nuclear stability. The results of this theory are given as a function of one parameter $\bar{z}$, the average charge displacement of the initial distribution from stability, which may be computed from the charge and mass of the target nucleus and the average neutron multiplicity $\bar{\nu}$. Griffin's results may be used to predict delayed gamma-ray intensities from photofission by replacing the mass A of the target nucleus by $A-1$ and using the appropriate value for $\bar{\nu}$ for photofission. Direct comparison of the present experimental results with theory is hindered by lack of experimental data on $\bar{\nu}$ for photofission; therefore, calculations of the delayed gamma-ray intensities were performed as a function of $\bar{\nu}$ for the three cases of photofission studied in this experiment. The results for the plateau time region, given as the rate of energy emission of all gamma rays having energies greater than 0.137 MeV, are shown in Fig. 11. The photon emission rates for the 0.51-MeV bias at t equal to approximately 10^{-2} sec, which are given in Table I and Fig. 10, were used for the comparison with the calculations. These data were converted to energy emission rates for a 0.137-MeV bias by means of the Fisher-Engle energy spectra of delayed gamma rays from the neutron fission of the corresponding target nuclei. The results, 1.18 ± 0.18 MeV/fission-sec for U^{238}, 0.42 ± 0.06 for U^{235}, and 0.61 ± 0.12 for Th^{232}, are shown in Fig. 11. Values of $\bar{\nu}$ covering the range from about 2.7 to 3.8 neutrons/fission adequately relate the delayed gamma-rays data to the calculations.

From the systematics of neutron fission and spontaneous fission presented by Leachman[14] and by Bondarenko *et al.*,[15] it is evident that $\bar{\nu}$ for the photofission of a given nuclide with a gamma ray having energy E_γ may be related to $\bar{\nu}$ for the spontaneous fission of the same nuclide by the expression

$$\bar{\nu}(E_\gamma)=\bar{\nu}_{\text{spontaneous}}+\alpha E_\gamma,$$

where α is almost independent of the fissioning nuclide and is approximately 0.14 MeV^{-1}. Assuming E_γ to be the energy at which the peak of the photofission cross section occurs (approximately 13 MeV for U^{238}, U^{235}, and Th^{232}) and taking values of $\bar{\nu}_{\text{spontaneous}}$ given by Bondarenko *et al.*,[15] one finds the following values of $\bar{\nu}$ for photofission: 3.6 neutrons/fission for U^{238}, 3.5 for U^{235}, and 3.2 for Th^{232}. As may be seen from Fig. 11, delayed gamma-ray intensities calculated with these values of $\bar{\nu}$ are consistent with the experimental data.

[14] R. B. Leachman, Proc. 2nd Intern. Conf. Peaceful Uses At. Energy **15**, 229 (1958).

[15] I. I. Bondarenko, B. D. Kuzminov, L. S. Kutsayeva, L. I. Prokhorova, and G. N. Smirenkin, Proc. 2nd Intern. Conf. Peaceful Uses At. Energy **15**, 353 (1958).

The present results for photofission overlap the measurements of Fisher and Engle[2] for times greater than 0.35 sec and those of Maienschein, Zobel, Peelle, and Love[3] for times greater than 1 sec. The latter measurements were performed for the case of thermal neutron fission of U^{235}, while the data of Fisher and Engle were obtained using a continuous spectrum of fast neutrons with a mean energy of 1.5 MeV. For comparison with present results, the data of these workers are given in Fig. 12, where the rates of gamma-ray energy emission per fission for gamma rays with energies greater than 0.28 MeV have been plotted. The Fisher-Engle data, which included all gamma rays with energies greater than 0.137 MeV, were adjusted to the low-energy limit (0.28 MeV) of the measurements of Maienschein *et al.* The photofission data were converted from photon emission rates to energy emission rates with the aid of the gamma-ray energy spectra measured by Fisher and Engle. The large differences in the intensities from photofission and from neutron fission are consistent with Griffin's theoretical correlation.

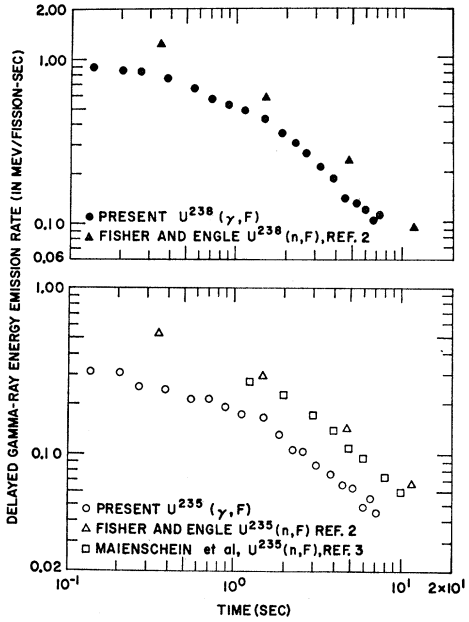

FIG. 12. Comparison of delayed gamma-ray intensities from photofission with results of others for neutron fission. All data are presented as rate of energy emission (MeV/fission-sec) for gamma rays having energies greater than 0.28 MeV.

Since only a few isomers contribute to the delayed gamma-ray intensity in the isomeric time region, a correlation procedure based on the average properties of a large number of fission products would be inappropriate for predicting intensities in this time region. For this reason, and because of the possible ambiguity in the present data from other competing photon reactions, measurements of delayed gamma rays in the isomeric region from neutron fission have been initiated at this

laboratory using the linear accelerator as a pulsed source of neutrons.

ACKNOWLEDGMENTS

We are grateful to Dr. J. R. Beyster for many helpful discussions throughout the course of the work, to the linear accelerator operating staff for their help with the beam, to W. D. Myers and D. H. Houston for aid in data reduction, to G. Buzzelli for the radiochemical analysis, and to W. M. Lopez for help with electronics. Thanks are due to Dr. J. Malik of Los Alamos Scientific Laboratory for arranging for the loan of the U^{235} samples and for his continued interest in the experiment. Discussions with Dr. J. Griffin, Dr. J. Malik, Dr. F. Maienschein, Dr. P. C. Fisher, and Dr. R. A. Schmitt were helpful.

PHYSICAL REVIEW VOLUME 134, NUMBER 4B 25 MAY 1964

Quantum Theory of Elementary Particles*

H. C. CORBEN

Thompson Ramo Wooldridge Space Technology Laboratories, Redondo Beach, California

(Received 21 November 1963; revised manuscript received 29 January 1964)

Quantum numbers which may possibly be identified with strangeness S, baryon number B, and isospin I are found to be natural consequences of the generalized field theory of a spinning particle developed in earlier papers, the theory requiring that $S+2I+2J$ is even, as observed. The generalized Dirac equation for fermions leads to the correct values of B, S, I_3, and J, and approximately the correct masses for the states n, p, Ξ^0, Ξ^-, $N_{13}{}^{*+}$, $N_{13}{}^{*0}$, the lowest known states of $I=\frac{1}{2}$, $J=\frac{1}{2}$, or $\frac{3}{2}$. The generalized Dirac equation for bosons similarly describes these quantities for the K and K^* mesons. The generalized Kemmer equation for fermions yields the correct values of B, S, I_3, J, and the masses for the Λ^0, $Y_0{}^*$, and $Y_{03}{}^*$ if the spin of the $Y_0{}^*$ is $\frac{1}{2}$, and the generalized Kemmer equation for bosons similarly leads to the correct masses, spins, and isospins for the $S=0$ states ϕ, f, ω, η, ρ, and predicts $I=1$, $S=0$ states at 1-BeV spin 1 (χ_1?), 1.24-BeV spin 2(B?), 450-MeV spin 0(ζ?), and $I=0$ states at 965 MeV (spin 1) and 926 MeV (spin 0). The only arbitrariness in the theory lies in the choice of the two mass parameters for each equation, and in the choice of which combination of two independently conserved currents allowed by each equation is identified with the electric current. The theory satisfies a correspondence principle with the classical relativistic equation of motion of a symmetric top, and yields a prescription for describing states of higher quantum numbers. It then predicts the spin of the $Y_0{}^{**}$ state as $\frac{5}{2}$, correctly describes the spin and mass of the $N_{15}{}^*$ state, predicts a series of N^* states 166 MeV apart of progressively increasing spin, and describes other states, the properties of which have not yet been investigated.

1. INTRODUCTION

IN our attempts to understand elementary particles and nuclear forces, for several decades we have been making an assumption that is not forced on us either by the principles of relativity theory or by the requirements of quantum theory. This assumption ultimately has to do with the *shape* of an elementary particle, but in the relativistic quantum theory of a point-particle, a concept such as shape does not enter. It is therefore necessary to examine the classical limit of relativistic field theory—the relativistic classical mechanics of a spinning particle—where the motion of the spin of even a point-particle can be described only when we know its moments of inertia about axes along, and perpendicular to, its spin axis. In the absence of any information about the structure of the particles it is necessary to treat the particle as a point with, however, a finite amount of spin-angular momentum associated with it. This requires nonzero moments of inertia if the angular velocity is to remain finite, and these may be prescribed as parameters which are a measure of the "shape" of the particle.

In the corresponding quantum theory we have ignored these questions, arguing that the angular velocity is not an observable and that it is sufficient to associate a spin-angular momentum with the particle, and look for equations of motion which lead to irreducible representations of the Lorentz group for different spin values. These equations, in particular those of Dirac and Kemmer, are also based on the assumption that the spin and rest mass of a particle are always constant parameters.

In view of the well-established correspondence between classical and quantum physics it seems surprising that dynamical variables and parameters such as angular velocity and moment of inertia, so important in classical mechanics, play no role in quantum theory. It has, therefore, seemed reasonable to conduct a reinvestigation of the relation between the Dirac equation and the classical equations of motion to see at what point the correspondence was lost. For many years it has

* Research Supported by the Company Independent Research Program of TRW Space Technology Laboratories and by the U. S. Office of Naval Research.